Journal of Statistical Physics, Vol. 82, Nos. 3/4, 1996

Superpositions of Multifractals: Generators of Phase Transitions in the Generalized Thermodynamic Formalism

Günter Radons[1] and Ruedi Stoop[2]

Received February 28, 1995

We investigate the superposition of multifractals in the generalized thermodynamic formalism. It is shown analytically that phase transitions of first and second order are obtained and that the topology of the corresponding critical lines endows bicritical behavior. We demonstrate that these phase transitions can be observed in the spectrum of fractal dimensions and in the spectra of related quantities. Therefore, the obtained results are of importance for the interpretation of experimental systems.

KEY WORDS: Multifractals; generalized thermodynamic formalism; projections of fractal measures; phase transitions.

1. INTRODUCTION

In many experimental situations it is impossible to observe the full multifractal structure of the object of interest since the desired information is only accessible in the form of projections. Examples are the observation of clouds, images of fractal structures in the universe, or, quite generally, of fractal structures with dimension larger than that of the image. For a multifractal analysis, to derive the consequences of such a situation constitutes a nontrivial theoretical problem. Correspondingly there exist only very few general results for this problem.[1-3] A related but simpler situation is obtained if one considers the superposition of two or more independent multifractals with measure. Such sums of multifractal measures, which can

[1] Institut für Theoretische Physik, Universität Kiel, D-24118 Kiel, Germany. E-mail: radons@theo-physik.uni-kiel.de.

[2] Institut für Theoretische Physik, Universität Zürich-Irchel, CH-8057 Zürich-Irchel, CH-8057 Zürich, Switzerland. E-mail: stoop@msp.chem.ethz.ch.

0022-4715/96/0200-1063$09.50/0

be regarded as a special case of the projection problem, give rise to nontrivial behavior even in the simplest case: In ref. 4 it is shown that sums of multifractal measures supported by the same equal-scale Cantor set lead to first- and unexpected second-order phase transitions[5–8] in the thermodynamics of multifractals.[9–14] Here we extend these results to the case of multiscale Cantor supports. The appropriate tool for the investigation of this more general case is the generalized or bivariate thermodynamic formalism as elaborated in refs. 15 and 16 and reviewed, e.g., in refs. 17 and 18.

2. RESULTS

In the following we consider sums of multifractal sources where all of the sources are complete, self-similar two-scale multifractals with multiplicative measures. One of these multifractals is then determined by the probabilities p_1, p_2 and the associated length scales l_1, l_2 (see, e.g., refs. 19 and 20). The hierarchical structure of this multiplicative process is captured in the generalized partition sum[11, 14–24]

$$Z_1(q, \beta, N) = (p_1^q l_1^\beta + (p_2^q l_2^\beta)^N \tag{1}$$

where N denotes the level of the construction hierarchy. The probabilities are normalized: $p_1 + p_2 = 1$. In order to label the M independent components we use the index ν. Accordingly, the system is characterized by the set of quantities $p_i(\nu)$, $l_i(\nu)$, where $i = 1, 2$ and $\nu = 1, ..., M$. In the following we investigate the case of the superposition μ of $M = 2$ multifractal measures $\mu(1)$ and $\mu(2)$, i.e., $\mu = \pi(1)\,\mu(1) + \pi(2)\,\mu(2)$, where the parameters $\pi(\nu)$ are the weights of the contributions of the involved multifractals $[\pi(1) + \pi(2) = 1]$. A further simplification is obtained if the supports of the two measures are the same. This implies that $l_i(1) = l_i(2) = l_i$ for all i. The partition sum of such a superposition then has the form

$$Z(q, \beta, N) = \sum_{j=0}^{N} \binom{N}{j} [\pi(1)\, p_1(1)^j\, p_2(1)^{N-j} + \pi(2)\, p_1(2)^j\, p_2(2)^{N-j}]^q \times (l_1^j l_2^{N-j})^\beta \tag{2}$$

In the following we assign without loss of generality the index $\nu = 1$ to the system with the larger value of p_1, i.e., $p_1(1) > p_1(2)$. In order to evaluate the partition sum of Eq. (2) in the limit of large N, we introduce the ratio $\xi = j/N$ and write Z as an integral

$$Z(q, \beta, N) \sim \int_0^1 e^{-Ng(\xi, q, \beta)}\, d\xi \tag{3}$$

For $\pi(1), \pi(2) \neq 0$ the function g is composed of two contributions:

$$g(\xi, q, \beta) = g_1(\xi, q, \beta)\, \theta(\xi - \xi_0) + g_2(\xi, q, \beta)\, \theta(\xi_0 - \xi) \tag{4}$$

with

$$g_\nu(\xi, q, \beta) = \xi \ln \xi + (1-\xi) \ln(1-\xi) \\ -\xi[q \ln p_1(\nu) + \beta \ln l_1] - (1-\xi)[q \ln p_2(\nu) + \beta \ln l_2] \tag{5}$$

where $\theta(x)$ denotes the step function and ξ_0 has the value

$$\xi_0 = \{1 + \ln[p_1(2)/p_1(1)]/\ln[p_2(1)/p_2(2)]\}^{-1} \tag{6}$$

This value is derived from the condition that the contributions from sources 1 and 2 to the partition sum are of the same order in the thermodynamic limit. With the saddle point approach the generalized free energy

$$\tau(q, \beta) = -\lim_{N \to \infty} \ln[Z(q, \beta, N)]/N \tag{7}$$

can be written as

$$\tau(q, \beta) = g(\xi(q, \beta), q, \beta) \tag{8}$$

where $\xi(q, \beta)$ maximizes the integrand in Eq. (3) by minimizing the function g for given q and β. Because of the simplicity of the model, it is straightforward to investigate the analyticity properties of the system. Quite surprisingly, nontrivial phase transition scenarios are detected. This is demonstrated in Fig. 1 where we show two typical phase diagrams in the q–β plane. It can be observed that there are three different domains in both situations. In each domain, $\tau(q, \beta)$ is analytic. The separation is by critical lines of first order (full lines in Fig. 1) or of critical lines of second order (dashed lines). At the intersection point B where two second-order phase boundaries merge into a first-order boundary, bicritical behavior[25, 26] is obtained, and B is called the bicritical point. In the following let us demonstrate these observations analytically. First, note that the value $\xi(q, \beta)$ which minimizes g determines $\tau(q, \beta)$ [cf. Eq. (8)]. We therefore concentrate on the location of the minimum of g. Since, according to Eq. (4), the function g is composed of two functions g_1 and g_2, we end up with three distinct cases: In the first case the minimum of g is provided by the minimum of g_1. Then $\tau(q, \beta)$ is equal to

$$\tau_\nu(q, \beta) = -\ln[p_1(\nu)^q\, l_1^\beta + p_2(\nu)^q\, l_2^\beta] \tag{9}$$

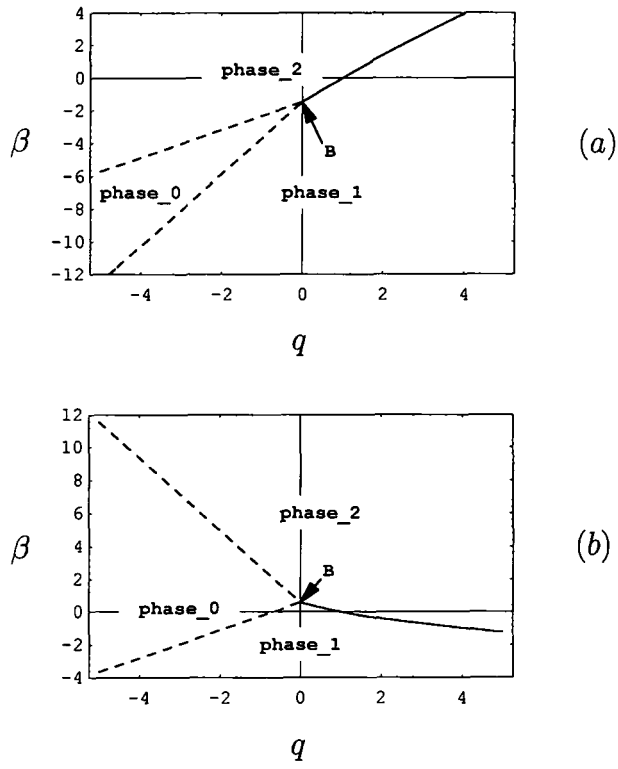

Fig. 1. Two typical phase diagrams for the superposition of two multifractal measures $\mu(1)$ and $\mu(2)$ [parameters: (a) $p_1(1)=0.9$, $p_1(2)=0.7$, (b) $p_1(1)=0.7$, $p_1(2)=0.1$]. Generically, there exist three phases which are separated by critical lines of first (full lines) and second order (dashed lines). Their intersection point B is a bicritical point. Note that the phase diagrams do not depend on l_1 and l_2 if β is measured in units of $\ln(l_2/l_1)$ [see Eqs. (11) and (12)]. Therefore, these units were used also in the following Figs. 2–7.

where $\nu=1$. Note that this expression is just the free energy of the isolated first source. The second case arises analogously, with $\nu=2$. There is, however, a third case, which occurs if the minimum is found at $\xi=\xi_0$ [Eq. (6)]. In this case, the location of the minimum is found at the intersection of the two branches g_1 and g_2; the corresponding $\tau_0(q,\beta)$ is given by

$$\tau_0(q,\beta)=g(\xi)|_{\xi=\xi_0} \tag{10}$$

All three cases are obtained in Fig. 1a if, for instance, the parameter q is held fixed at $q=-1$ and β assumes the values $\beta=-2$, 1, and 4, respectively. Figure 2 shows the corresponding pictures of the free energy

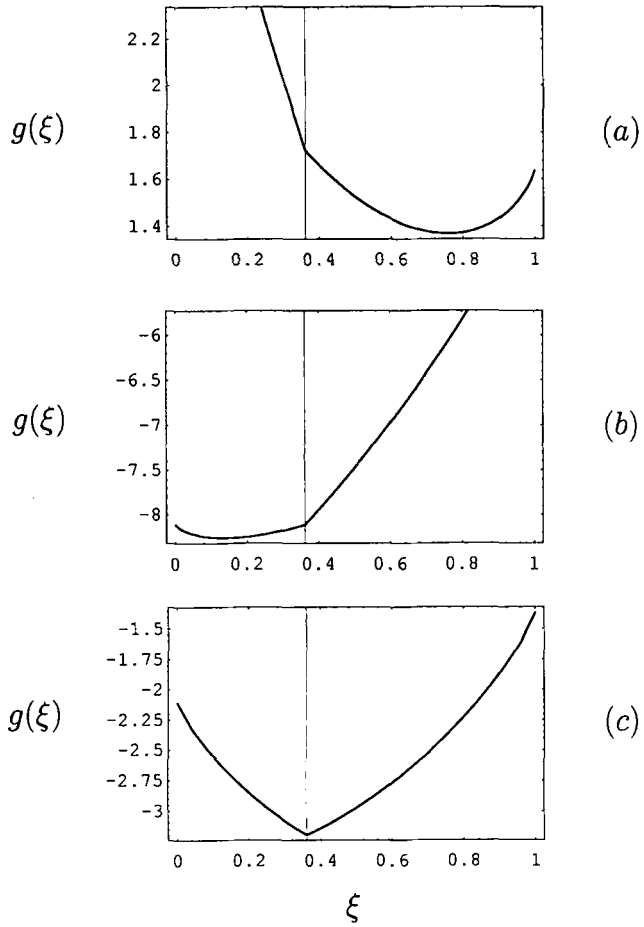

Fig. 2. The free energy functional $g(\xi, q, \beta)$, Eq. (4), for each of the three phases on the line $q = -1$. (a) $\beta = -2$: A minimum on the right of the vertical line (located at $\xi_0 = 0.3608...$ [see Eq. (6)] means that the system is in *phase_1* corresponding to multifractal measure $\mu(1)$ (b) $\beta = 4$: The minimum is left of ξ_0, meaning that the system is in *phase_2* where measure $\mu(2)$ dominates. (c) A new *phase_0* appears if the minimum is at ξ_0, e.g., for $\beta = 1$ (parameters as in Fig. 1b with $l_1 = 1/3$, $l_2 = 1/9$).

functionals g. In the following we derive where the phase transitions occur as a function of the variables q, β and we work out the order of the transitions. By a continuous variation of parameter β we arrive at the situations shown in Fig. 3. They are characteristic for the transition between *phase_1* and *phase_0* and between *phase_0* and *phase_2*, respectively. It is now

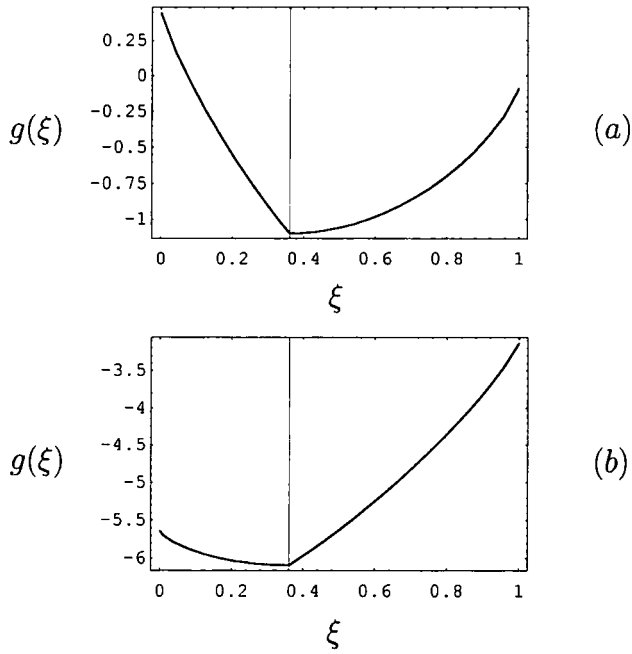

Fig. 3. Same as Fig. 2, with β chosen to hit second-order critical lines. (a) $\beta = \beta_{01}$: the minimum of $g_1(\xi, q, \beta)$ coincides with ξ_0; (b) $\beta = \beta_{02}$: $\arg\min_\xi g_2(\xi, q, \beta) = \xi_0$.

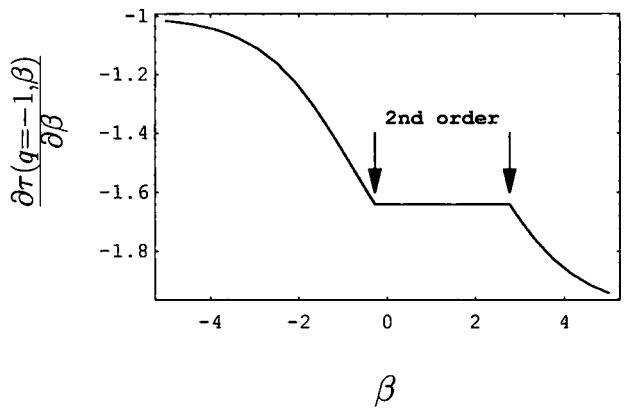

Fig. 4. The first derivative of the generalized free energy $\partial\tau(q, \beta)/\partial\beta|_{q=-1}$ is continuous at the critical points $\beta_{01}(q=-1)$ and $\beta_{02}(q=-1)$, but discontinuous in the second derivative. This shows that here the phase transitions are of second order [parameters $p_i(v)$, l_i as in Fig. 2].

important to note that the phase boundaries $\beta_{\nu\bar{\nu}}(q)$ between the phases ν and $\bar{\nu}$ are obtained from the conditions $\tau_\nu(q, \beta) = \tau_{\bar{\nu}}(q, \beta)$. From this it is easily found that

$$\beta_{0,\nu}(q) = -\left(\ln \frac{\ln[p_1(1)/p_1(2)]}{\ln[p_2(2)/p_2(1)]} + q \ln \frac{p_1(\nu)}{p_2(\nu)} \right) \Big/ \ln \frac{l_1}{l_2} \tag{11}$$

where $\nu = 1, 2$. The order of the phase transitions is determined by the derivates of the free energy $\tau(q, \beta)$. In Fig. 4, we again keep q fixed at the

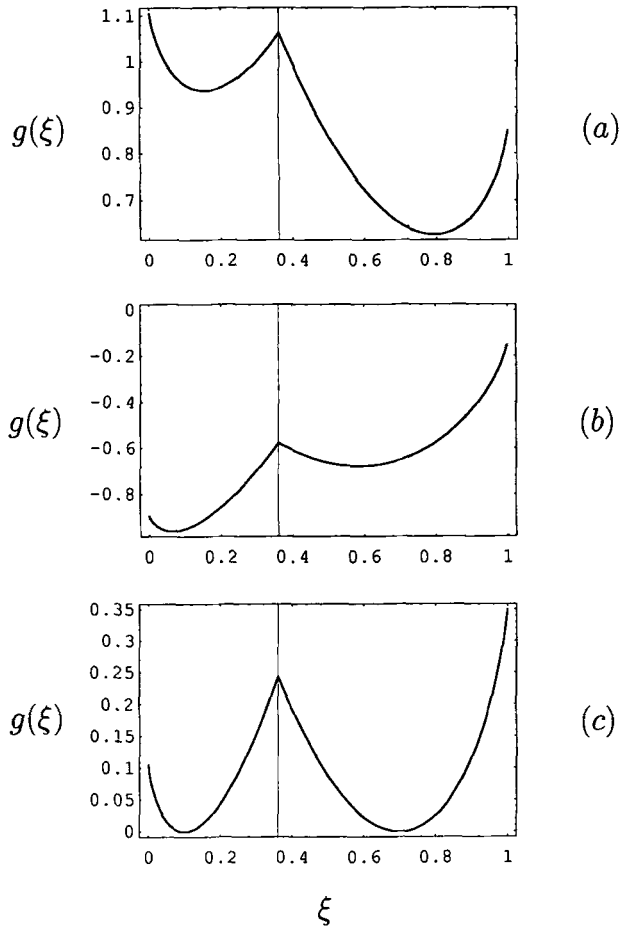

Fig. 5. Same as Fig. 2, but for $q = 1$ and (a) $\beta = -0.5$, (b) $\beta = 0.5$, and (c) $\beta = \beta_{12} = 0$. Obviously the "order parameter" $\xi_{\min}$ jumps at the transition from (a) to (b) via (c). This first-order behavior is verified in Fig. 6.

value $q = -1$ and plot the analytically derived first derivative of τ with respect to β as we cross the phase border upon variation of β. The continuity of the first derivative and the apparent jump in the second derivative clearly identify a second-order phase transition. The very same situation holds for the whole left half-plane $q < 0$.

On the right half-plane, however, a direct transition between *phase_1* and *phase_2* is found. The corresponding phase boundary is given by

$$\beta_{1,2}(q) = -\left(\ln \frac{p_1(1)^q - p_1(2)^q}{p_2(2)^q - p_2(1)^q}\right) \Big/ \ln \frac{l_1}{l_2} \tag{12}$$

In Fig. 5 we show the free energy functional g below, above, and at the critical line $\beta_{1,2}(q)$. Again, the minimum of g determines the free energy τ. From the plots it is clear that the location of the minimum (which plays the role of the order parameter) jumps as the critical line is crossed. This typical first-order behavior is accordingly verified in Fig. 6, where one finds that the first derivative of τ with respect to β jumps upon variation of β as we cross the phase boundary along the line $q = 1$.

Clearly, phase transitions are important features by themselves. They gain, however, even more importance if they can be connected with observations from experiments. In experiments, usually the generalized dimensions[10, 27] D_q or the spectrum of dimensions[11] $f(\alpha)$ is measured. D_q can be obtained from the zeros of the generalized free energy $\tau(q, \beta(q)) = 0$ as $D_q = -\beta(q)/(q-1)$.[17] The function $-\beta(q)$ is usually denoted by $\tau(q)$ and its Legendre transform is the spectrum of dimensions $f(\alpha)$. The point of interest is whether the phase transition detected above have an effect on these functions. We therefore concentrate on the level line $\tau(q, \beta) = 0$. In

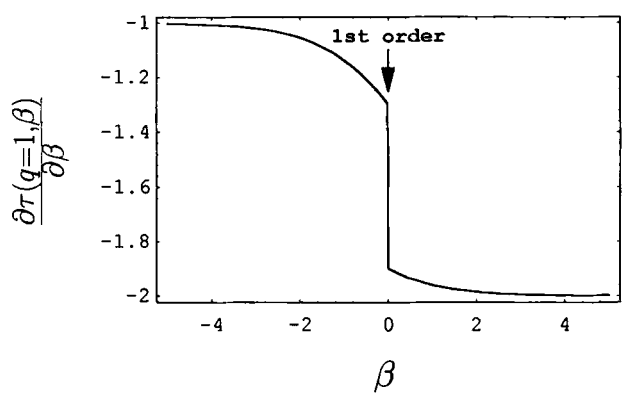

Fig. 6. Same as Fig. 4, but on the line $q = 1$.

the contour plots of Fig. 7, this line can easily be identified. In both pictures, the zero-level line crosses the first-order phase boundary at the point $(q_{1st}, \beta_{1st}) = (1, 0)$. This is true in general, since trivially $\tau(q) = (q-1) D_q$ is zero for $q = 1$, and from Eq. (12), $\beta_{1,2}(q=1) = 0$. Therefore, the first-order phase transition is always detected in experiments to which our theoretical setting applies. In contrast, the presence of the second-order phase

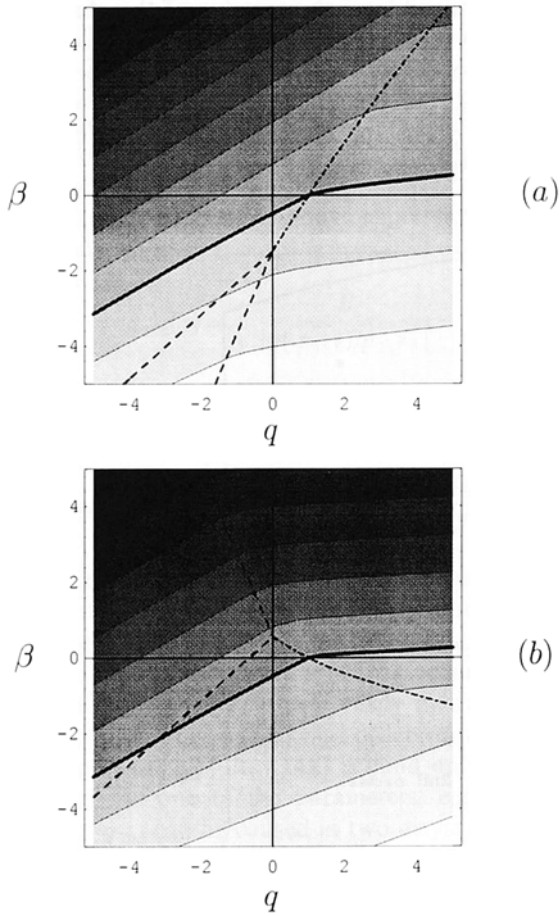

Fig. 7. Contour lines ($\Delta\tau = 2$) of the generalized free energy $\tau(q, \beta)$ for the cases of Fig. 1 and for $l_1 = 1/3$, $l_2 = 1/9$. The zero-level line (full line) is the well-known free energy $\tau(q)$ of ref. 11. The first- and second-order phase transitions show up in the latter curves as crossings with the critical lines (dashed, same as in Fig. 1): (a) ($p_1(1) = 0.9$, $p_1(2) = 0.7$) yields a first-order transition only, (b) ($p_1(1) = 0.7$, $p_1(2) = 0.1$) yields a first- and a second-order phase transition in $\tau(q)$.

transition may or may not be observable in $\tau(q)$, depending on the system parameters. This is clearly seen in Fig. 8, where the first derivative $\partial\tau(q)/\partial q$ is depicted for the two cases shown in Fig. 7.

In the following we derive analytically the critical q value q_{2nd} where the second derivative of $\tau(q)$ is discontinuous. From this result we will be able to find the parameter regime where the second-order phase transition is observable. In order to calculate the critical value q_{2nd}, we observe that this value can determined from the crossing of the phase boundary $\beta_{0\nu}(q)$ for $\nu=1$ or $\nu=2$ by the zero-level line $\beta=-\tau_\nu(q)$ of $\tau_\nu(q,\beta)$. Although there is in general no explicit analytical expression for the solution of the equation $\tau_\nu(q,\beta)=0$, the defining equation $\tau_\nu(q,\beta=\beta_{0\nu}(q))=0$ can be solved for q, which yields the desired solution q_{2nd} provided that $q\leqslant 0$. Proceeding in this way, one obtains that

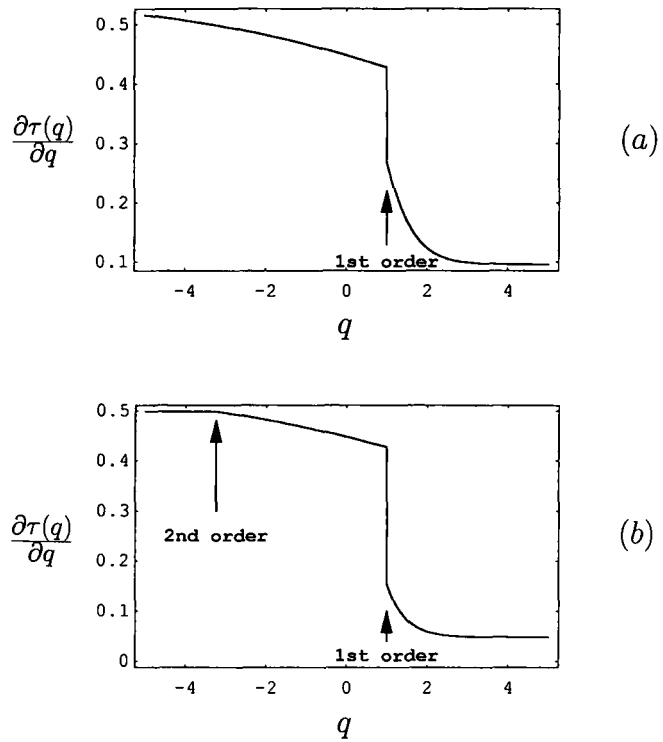

Fig. 8. For the two cases of Fig. 7 we show plots of the analytic results for the derivative $\partial\tau(q)/\partial q$. In both cases a jump is observable. The discontinuity in the second derivative, however, appears only in the case corresponding to Fig. 7b.

$$q_{2\mathrm{nd}}(\nu) = -\frac{\tilde{B}\ln\tilde{l} + \ln[1+\exp(\tilde{B})]}{\ln p_1(\nu) + \ln\tilde{l}\cdot\ln[p_1(\nu)/p_2(\nu)]} \tag{13}$$

where

$$\tilde{B} = \ln\frac{\ln[p_1(1)/p_1(2)]}{\ln[p_2(2)/p_2(1)]} \qquad \text{and} \qquad \ln\tilde{l} = \left(\frac{\ln l_2}{\ln l_1} - 1\right)^{-1}$$

Depending on whether the transition is from *phase_1* to *phase_0* or from *phase_2* to *phase_0*, the value $\nu = 1$ or $\nu = 2$, respectively, has to be taken. $\tilde{B}$ is the β value of the bicritical point in units of $\ln l_2/\ln l_1$ [cf. Eqs. (11), (12)] and $\tilde{l}$ is recognized as an effective length scale if $\tau_\nu(q, \beta)$ is expressed in these rescaled coordinates. This means that in order to determine $q_{2\mathrm{nd}}$, the original length scales l_1 and l_2 are not explicitly needed, since only the combination $\ln l_2/\ln l_1$ appears in the above expression. In the limit $l_1 \to l_2$ the expression simplifies to

$$q_{2\mathrm{nd}}(\nu) = -\frac{\tilde{B}}{\ln[p_1(\nu)/p_2(\nu)]}$$

a result which has been obtained previously.[4] Equation (13) can be rewritten in a more symmetrical form as

$$q_{2\mathrm{nd}}(\nu) = \left(\frac{1}{\ln l_1} - \frac{1}{\ln l_2}\right)\frac{\tau(q=0, \beta=\beta_{\lambda\tilde{\lambda}}(q=0))}{\ln p_1(\nu)/\ln l_1 - \ln p_2(\nu)/\ln l_2} \tag{14}$$

The numerator τ in this equation represents just the generalized free energy at the bicritical point. Equation (14) is more easily obtained from the intersection of the zero level of $\tau_0(q, \beta)$ with the phase boundaries $\beta_{0\nu}(q)$, which is an alternative but equivalent criterion for the occurrence of the second-order phase transition. From the latter it easily inferred that at most one intersection and therefore only one second-order transition is possible. As before, the expression for $q_{2\mathrm{nd}}$ [Eq. (14)] is valid only as long as negative values are produced. As one of the parameters, e.g., $p_1(1)$, is varied, a change in the sign of $q_{2\mathrm{nd}}$ can be caused in two ways: either by a transition through the pole, determined by

$$\frac{\ln p_1(\nu)}{\ln l_1} = \frac{\ln p_2(\nu)}{\ln l_2} \tag{15}$$

or by a change of the sign of the generalized free energy at the bicritical point. For the latter to take place, the bicritical point has to cross the zero-level line of $\tau(q, \beta)$. While doing so, the analytical form $q_{2\mathrm{nd}}(1)$ changes to

$q_{2nd}(2)$. These scenarios are illustrated in Fig. 9a, where $p_1(1)$ is varied in the interval $[0, 1]$ for fixed $p_1(2) = 0.4$ and $l_2 = l_1^2$. As a simple consequence of this scenario, we may conclude that the boundaries which determine the onset of the occurrence of the second-order phase transition in the parameter space are simply given by Eq. (15) with $\nu = 1$ and $\nu = 2$. Note that this equation can also be expressed as $D_{-\infty}(\nu) = D_{\infty}(\nu)$, where $D_{\pm\infty}(\nu)$ are the asymptotic slopes of the functions $\tau_\nu(q)$.[11] These conditions are best understood in connection with the results for the $f(\alpha)$ spectra discussed

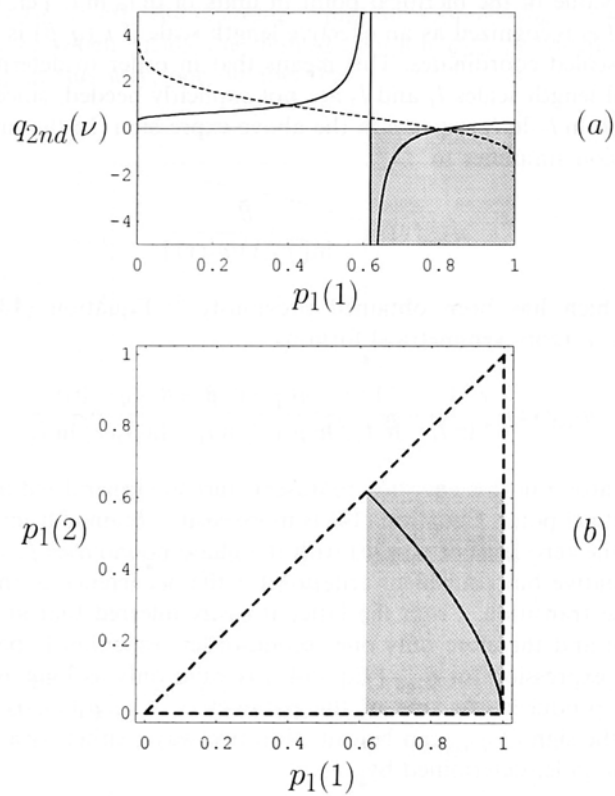

Fig. 9. (a) The q value at which $\tau_\nu(q)$ and the corresponding critical line $\beta_{0\nu}(q)$ intersect is plotted as a function of $p_1(1)$ for $\nu = 1$ (full line) and $\nu = 2$ (dashed line). In the parameter region (gray shaded) where the intersection occurs at negative q values, q is identical with the critical value q_{2nd}. (b) In the symmetry-reduced $p_1(1)$–$p_1(2)$ parameter regime (dashed triangle) there exists a rectangle R, Eq. (16), where the second-order phase transition is observable (gray shaded). On the solid line the numerator of Eq. (13) vanishes. It separates the parameter regimes where the expressions for $q_{2nd}(1)$ and $q_{2nd}(2)$ are valid, respectively.

below. For given l_1 and l_2, Eq. (15) is a transcendental equation for $p_1(v)$ [since $p_2(v) = 1 - p_1(v)$]. Denoting the larger of the solutions by p^*, one obtains as the parameter regime for the existence of the second-order phase transition the rectangle

$$R = [p^* \leqslant p_1(1) \leqslant 1] \times [0 \leqslant p_1(2) \leqslant p^*] \tag{16}$$

[remember that by symmetry we may restrict ourselves to $p_1(1) \geqslant p_1(2)$]. Thus, for any combination of length scales l_1, l_2, there exists a regime in the $p_1(1)$–$p_1(2)$ plane where a second-order transition occurs. For $l_2 = l_1^2$ (which has been used in the previous figures) one obtains $p^* = (\sqrt{5} - 1)/2$. This region, together with the line where the analytic form for q_{2nd} changes from $q_{2nd}(1)$ to $q_{2nd}(2)$, is depicted in Fig. 9b.

The effect of these phase transitions is more drastically exhibited in the function $f(\alpha)$, the Legendre transform of $\tau(q)$[11], which will allow us to gain a deeper insight into the mechanisms leading to the phase transitions. Figure 10 shows the $f(\alpha)$ curves corresponding to the cases of Fig. 7. Whereas the first-order phase transition is detected in both figures as a straight-line segment,[28] the second-order phase transition (present only in Fig. 7b) is observed as a stopping point in the $f(\alpha)$ curve with *finite* left-hand derivative. Note that the stopping point at $\alpha = \alpha_{max}$ is identical with the intersection point of the curves $f_1(\alpha)$ and $f_2(\alpha)$ which correspond to the isolated measures $\mu(1)$ and $\mu(2)$, respectively. This fact is characteristic for the observed second-order phase transition. In order to make this point clear we consider the scaling behavior of the isolated measures $\mu(1)$, $\mu(2)$, respectively. Let us denote by $\alpha_v(\xi)$ the scaling exponent (Hölder exponent) of the measure $\mu(v)$ restricted to the fractal subset $S(\xi)$ of the support S of μ, where ξ is some real number in the interval $[0, 1]$ (recall that [cf. Eqs. (2), (3)] $j = \xi N$ is the number of digits one in the binary addresses of the fractal elements.[19] For the two-scale Cantor measure, $\alpha_v(\xi)$ is given by[11]

$$\alpha_v(\xi) = \frac{\xi \ln p_1(v) + (1 - \xi) \ln p_2(v)}{\xi \ln l_1 + (1 - \xi) \ln l_2} \tag{17}$$

The fractal dimension (Hausdorff dimension) of $S(\xi)$ is given by

$$f(\xi) = \frac{\xi \ln \xi + (1 - \xi) \ln(1 - \xi)}{\xi \ln l_1 + (1 - \xi) \ln l_2} \tag{18}$$

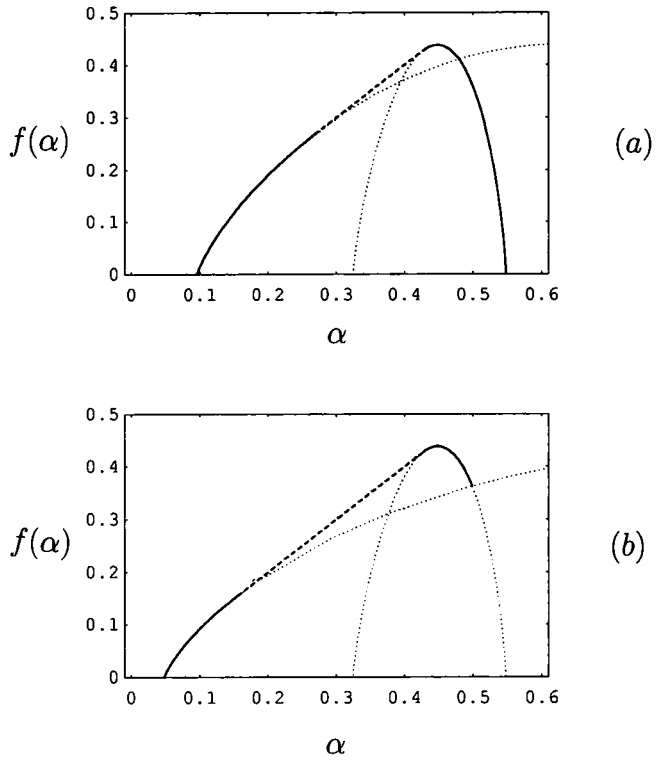

Fig. 10. The Legendre transforms $f(\alpha)$ (full line) of the functions $\tau(q)$ of Fig. 7 are known analytically. The first-order transition appears as a straight-line segment (dashed) on the bisectrix $f(\alpha)=\alpha$ [in (a) and (b)]. The second-order transition is recognized as a stopping point of $f(\alpha)$ with a finite slope at $\alpha_{\max}$ case (b)]. The stopping point is identical with the intersection point of the curves $f_1(\alpha)$ and $f_2(\alpha)$ (dotted lines) corresponding to the separate measures $\mu(1)$ and $\mu(2)$.

The curves $f_\nu(\alpha)$ are then obtained by solving Eq. (17) for ξ and inserting this expression into Eq. (18), which yields

$$f_\nu(\alpha)=f\left(\xi=\frac{\ln p_2(\nu)-\alpha \ln l_2}{\ln[p_2(\nu)/p_1(\nu)]-\alpha \ln(l_2/l_1)}\right) \tag{19}$$

Now remember that the *phase_0* is characterized by the unique value $\xi=\xi_0$, Eq. (6), where the two contributions in Eq. (2) are asymptotically of the same order. The latter condition can also be written as $\alpha_1(\xi_0)=\alpha_2(\xi_0)$, and $\tau_0(q)$, the zero-level line of $\tau_0(q,\beta)$ of Eq. (10), can be expressed as $\tau_0(q)=q\cdot\alpha_\nu(\xi_0)-f(\xi_0)$. This shows that at the transition to

phase_0, the scaling exponents $\alpha_0 \equiv \partial\tau_0(q)/\partial q = \alpha_1(\xi_0) = \alpha_2(\xi_0) = \alpha_{\max}$ coincide. Also the fractal dimensions are identical and equal to $f(\xi_0)$. We emphasize, however, that the intersecting of the 'unperturbed' curves $f_\nu(\alpha)$ is not a sufficient condition for the occurrence of the second-order phase transition [the $f(\alpha)$ curves of the isolated measures $\mu(\nu)$ intersect also in the case of Fig. 10a, but no second-order transition is observed]. In addition, the parameters have to lie in the rectangle R of Eq. (16). The latter condition basically expresses a *geometrical* relationship between the measures $\mu(1)$ and $\mu(2)$. In order to see this we show in Fig. 11 the functions $\alpha_\nu(\xi)$, $\nu = 1, 2$, of Eq. (17) for case (a) where only a first-order transition is present, and for case (b) where in addition the second-order

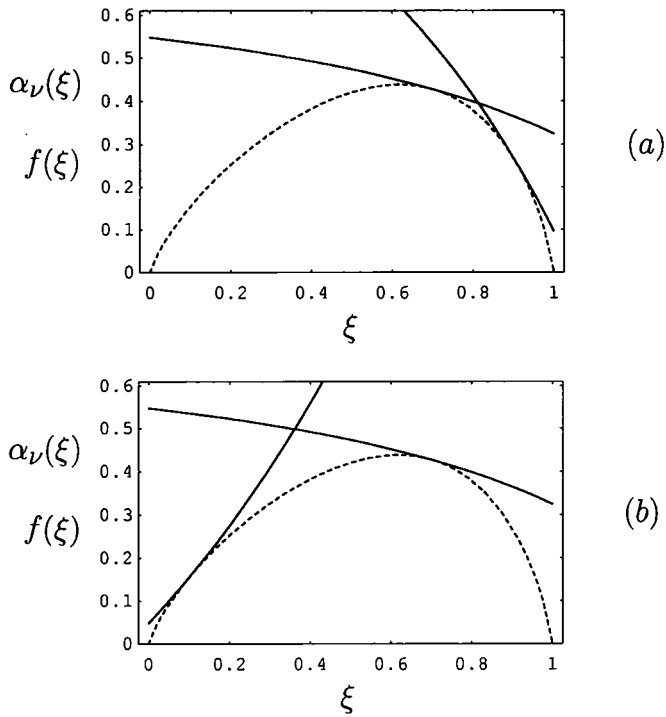

Fig. 11. The functions $\alpha_\nu(\xi)$, $\nu = 1, 2$, are shown as full lines, together with $f(\xi)$ from Eq. (18) (dashed). The singularity exponent $\alpha(\xi) = \min_\nu \alpha_\nu(\xi)$ is monotonous in case (a), whereas in case (b) it exhibits a maximum at the intersection point ξ_0. The latter fact is the reason for the second-order phase transition. For a given value of α [in the range of $\alpha(\xi)$], the value $f(\alpha)$ is found by taking the preimage ξ of α under the mapping $\alpha(\xi)$ and reading off the corresponding value $f(\xi)$. If there are two preimages [possible only in case (b)], the value with the larger $f(\xi)$ has to be taken. However, this construction is not valid in the α range between the two tangencies of $\alpha(\xi)$ with $f(\xi)$, since $f(\alpha) = \alpha$ in this region (first-order phase transition).

transition is observable. First note that $\alpha_\nu(\xi)$ is always a monotonous function of ξ, since

$$\frac{\partial \alpha_\nu(\xi)}{\partial \xi} = \frac{\ln l_1 \cdot \ln l_2}{[\xi \ln l_1 + (1-\xi)\ln l_2]^2} \cdot \left(\frac{\ln p_1(\nu)}{\ln l_1} - \frac{\ln p_2(\nu)}{\ln l_2} \right) \tag{20}$$

is either positive or negative, depending on the sign of the second factor in Eq. (20). Taking into account the results of Fig. 11, this means that in case (a) the measures are superimposed such that the strongest singularities $\min_\xi(\alpha_\nu(\xi))$ of both measures $\mu(\nu)$, $\nu = 1, 2$, lie on the same set $S(\xi = 1)$ and also the weakest singularities $\max_\xi(\alpha_\nu(\xi))$ add up on the same set $S(\xi = 0)$. In contrast, for case (b) the superposition is such that $\min_\xi(\alpha_1(\xi))$ and $\max_\xi(\alpha_2(\xi))$ are combined on $S(\xi = 1)$, and $\max_\xi(\alpha(\xi))$ is combined with $\min_\xi(\alpha_2(\xi))$ on the set $S(\xi = 0)$. In order to see that this argument actually explains the $f(\alpha)$ spectra of Fig. 10 and therefore the phase transitions encountered, one has to compute the singularity exponents $\alpha(\xi)$ of the combined measure $\mu(1) + \mu(2)$. By the same reasoning that leads to Eq. (2), one finds

$$\begin{aligned} \alpha(\xi) &= \lim_{N \to \infty} \frac{\ln[\pi(1)\, p_1(1)^{\xi N} p_2(1)^{(1-\xi)N} + \pi(2)\, p_1(2)^{\xi N} p_2(2)^{(1-\xi)N}]}{\ln(l_1^{\xi N} l_2^{(1-\xi)N})} \\ &= \min \alpha_\nu(\xi) \end{aligned} \tag{21}$$

This equation is the key for explaining the form of the $f(\alpha)$ curves in our model. It implies that in case (a) possible α values are restricted to the interval $[\alpha(\xi = 1), \alpha(\xi = 0)]$. In case (b), however, they are confined to the interval $[\alpha(\xi = 0), \alpha(\xi = \xi_0)]$, since here the maximum is attained at the cusp at $\xi = \xi_0$. This means that the fractal dimension which corresponds to this point is $f(\xi_0) > 0$, as can be read off in Fig. 11 from the function $f(\xi)$ (dashed line). This is in contrast to case (a), which yields the usual result $f(\xi = 0) = f(\xi = 1) = 0$. This explains exactly the behavior of the $f(\alpha)$ spectra shown in Fig. 10.

With this improved understanding of the phase transition behavior we may now formulate a necessary and sufficient condition for the occurence of a transition of second order. This transition occurs iff the function $\alpha(\xi)$ attains its maximum on the open interval $(0, 1)$, which is only possible if one of the functions α_ν is decreasing while the other is increasing. With the aid of Eq. (20), this can be stated as

$$\left(\frac{\ln p_1(1)}{\ln l_1} - \frac{\ln p_2(1)}{\ln l_2} \right) \left(\frac{\ln p_1(2)}{\ln l_1} - \frac{\ln p_2(2)}{\ln l_2} \right) \leqslant 0 \tag{22}$$

This, of course, defines the same rectangle R [and its equivalent mirror image for $p_1(1) < p_1(2)$] as is given by Eq. (16). Noting that Eq. (22) can also be written as $[\alpha_1(0) - \alpha_2(0)][\alpha_1(1) - \alpha_2(1)] \leqslant 0$, one observes that at the boundaries of R, one of the multifractal measures $\mu(\nu)$ actually degenerates to a simple fractal measure, characterized by a single singularity exponent $\alpha = D_{-\infty}(\nu) = D_{\infty}(\nu)$ and a single fractal dimension.

In conclusion we mention that the inverse Legendre transform of $f_\nu(\alpha)$ of Eq. (19) yields a parametrical representation of $\tau_\nu(q)$, the zero level of $\tau_\nu(q, \beta)$ of Eq. (9). It is given by $\tau_\nu(\alpha) = \alpha\, \partial f_\nu(\alpha)/\partial_\alpha - f_\nu(\alpha)$ and $q_\nu(\alpha) = \partial f_\nu(\alpha)/\partial_\alpha$ [for the choice of parameters $l_2 = l_1^2$ used in the figures there exists also an explicit formula for $\tau_\nu(q)$]. Thus, with the results presented above, we have obtained a full analytical solution for the problem of the superposition of two two-scale Cantor measures and the resulting phase transition scenarios.

3. DISCUSSION

The basic nature of the system investigated suggests that this kind of phase transition behavior can also be observed in experiments. It is well possible that in the light of our results the unexpected behavior of some experimental systems can be explained in a novel and very natural way. Although we have restricted our presentation to the superposition of two two-scale multiplicative measures, the discussed phenomena are more general. In ref. 4, for instance, it has been shown that the inclusion of memory in the construction hierarchy (Markovian instead of multiplicative measures) leads to the same type of phase transitions. In the equal-scale situation treated there one also has an interpretation of the observed phase transitions in terms of a simple one-dimensional Ising system with long-range interactions. From our discussion of the $f(\alpha)$ curves it follows that an extension to more than two measures and more than two scales yields similar results. In particular, the possibility for second-order transitions to new thermodynamic phases exists also in these very general cases. Finally, from a theoretical point of view, it is interesting to note that the treatment presented here provides us with one of the few known mechanisms (for alternatives see ref. 29) for second-order phase transitions in the thermodynamics of multifractals.

ACKNOWLEDGMENTS

R.S. acknowledges the generous support by D. Wyler and the Swiss National Science Foundation. We are indebted to one of the referees for bringing ref. 5 to our attention.

REFERENCES

1. P. Mattila, *Ann. Acad. Sci. Fenn. A I* **1**:227 (1975).
2. G. Radons, *Physica A* **191**:532 (1992).
3. G. Radons, *J. Stat. Phys.* **72**:227 (1993).
4. G. Radons, *Phys. Rev. Lett.* **75**:2518 (1995).
5. O. E. Lanford, in *Statistical Mechanics and Mathematical Problems*, A. Lenard, ed. (Springer, Berlin, 1973).
6. D. Katzen and I. Procaccia, *Phys. Rev. Lett.* **58**:1169 (1986).
7. P. Grassberger, in *Proceedings Workshop on Dynamics on Fractals and Hierarchies of Critical Exponents* (Orsay, 1986).
8. P. Cvitanović, in *XVth International Colloquium on Group Theoretical Methods in Physics*, R. Gilmore, ed. (World Scientific, Singapore, 1987).
9. D. Ruelle, *Thermodynamic Formalism* (Addison-Wesley, Reading, Massachusetts, 1978).
10. H. G. E. Hentschel and I. Procaccia, *Physica* **8D**:435 (1983).
11. T. C. Halsey, M. H. Jensen, L. P. Kadanoff, I. Procaccia, and B. Shraiman, *Phys. Rev. A* **33**:1141 (1986).
12. J. P. Eckmann and I. Procaccia, *Phys. Rev. A* **34**:659 (1986).
13. H. G. Schuster, *Deterministic Chaos*, 2nd ed. (VCH, Weinheim, 1989).
14. T. Tél, *Z. Naturforsch.* **43a**:1154 (1988).
15. R. Stoop, *Z. Naturforsch* **46a**:1117 (1991).
16. Z. Kovács and T. Tél, *Phys. Rev. A* **45**:2270 (1992).
17. J. Peinke, J. Parisi, O. E. Roessler, and R. Stoop, *Encounter with Chaos* (Springer, Berlin, 1992).
18. Ch. Beck and F. Schögl, *Thermodynamics of Chaotic Systems* (Cambridge University Press, Cambridge, 1993).
19. J. Feder, *Fractals* (Plenum Press, New York, 1988).
20. K. Falconer, *Fractal Geometry* (Wiley, Chichester, 1990).
21. M. Kohmoto, *Phys. Rev. A* **37**:1345 (1988).
22. R. Stoop and J. Parisi, *Phys. Rev. A* **43**:1802 (1991).
23. R. Stoop, J. Parisi, and H. Brauchli, *Z. Naturforsch* **46a**:642 (1991).
24. R. Stoop and J. Parisi, *Phys. Lett. A* **161**:67 (1991).
25. M. E. Fisher and D. R. Nelson, *Phys. Rev. Lett.* **32**:1350 (1975).
26. W. Gebhardt and U. Krey, *Phasenübergänge und kritische Phänomene* (Vieweg, Braunschweig, 1980).
27. P. Grassberger and I. Procaccia, *Phys. Rev. Lett.* **50**:346 (1983).
28. E. Ott, C. Grebogi, and J. A. Yorke, *Phys. Lett. A* **135**:343 (1989).
29. G. Radons, *Z. Naturforsch* **49a**:1219 (1994).